Polymer Degradation and Stability 220 (2024) 110631

Contents lists available at ScienceDirect

Polymer Degradation and Stability

journal homepage: www.journals.elsevier.com/polymer-degradation-and-stability

Influence of γ–radiation input dose and post-radiation high temperature shear grinding on polypropylene functional group composition

Sadulla R. Allayarov [a,*], Matthew P. Confer [b,c], Tatyana N. Rudneva [a], Sergei V. Demidov [a], Vadim G. Nikolskii [d], Svetlana D. Chekalina [a], David A. Dixon [b,*]

[a] Federal Research Center of Problems of Chemical Physics and Medicinal Chemistry of the Russian Academy of Sciences, Chernogolovka 142432, Russia
[b] Department of Chemistry and Biochemistry, Shelby Hall, The University of Alabama, Tuscaloosa, AL 35487-0336, USA
[c] Beckman Institute for Advanced Science and Technology, University of Illinois Urbana-Champaign, Urbana, IL 61801, USA
[d] N.N. Semenov Federal Research Center for Chemical Physics of the Russian Academy of Sciences, Moscow 119991, Russia

ARTICLE INFO

Keywords:
Polypropylene
γ-irradiation
High-temperature shear grinding
IR spectroscopy
Radiation oxidation
Correlated G3(MP2)B3 molecular orbital theory
Predicted decomposition thermodynamics

ABSTRACT

The effect of γ-irradiation in vacuum and air followed by HTSG of polypropylene (PP) is studied using both infrared (IR) spectroscopy and computational chemistry at the correlated G3(MP2)B3 molecular orbital theory level. γ-irradiation of PP in vacuum was found to primarily induce unsaturation and hydroxyl formation from residual system water whereas γ-irradiation of PP in air oxidizes the polymer and degrades the backbone in a thin layer due to oxygen permeability limitations as supported by the computational thermodynamics results. HTSG of the irradiated PP produced smaller particles than un-irradiated PP. HTSG of the irradiated PP led to a decrease in the IR band intensity from degradation due to a nominal homogenization of the pellet. HTSG of air irradiated PP led to a reduction in IR vibrational band intensity from oxidation due to thermal degradation. High-temperature shear grinding of γ-irradiated PP produces variable chemical and physical composition depending on irradiation input dose and environmental conditions. The combination of γ-irradiation and HTSG may be of benefit in recycling polypropylene.

1. Introduction

Polypropylene (PP) is the second most common synthetic plastic from the polyolefin family after polyethylene (PE), and is actively used across all sectors of the economy, including automotive, electronics, instruments, construction, etc. [1–3]. Many of PP's important physical properties are due to the molecular and supramolecular structure of the polymer chain, which is more complex than in PE due to the presence of the CH_3 side chain group. As a result, PP can exist in three stereoisomers: syndiotactic, isotactic, and atactic, which are obtained by different orientations of the monomer leading to different physicochemical properties [1–3]. The most important type of PP is the isotactic isomer characterized by a high degree of crystallinity, high strength, hardness and heat resistance. The atactic fraction of PP is unable to crystallize due to its inherent disordered structure and has poor mechanical properties. Atactic PP is an undesirable impurity in commercial PP produced using Ziegler-Natta catalysts. The isotactic fraction of PP dominates in the composition of the synthesized polymer. The physical and chemical properties of PP are thus dependent not only on the types of stereoisomers present but also their ratios. The processing of PP by different methods has a significant impact on the properties of the finished products.

Although the methods for processing of PP and other polyolefins and composites are well-established [4,5], there are a number of problems associated with the disposal of the polymer waste [6]. PP waste can be treated by pyrolysis, gasification, combustion, mechanical and chemical means. In order to minimize environmental impact, pyrolysis is currently preferred over gasification [7,8]. High-temperature shear grinding (HTSG) using rotary dispersers has been proposed as a method for recycling polymers including synthetic rubber [9]. Such grinding based on the principle of Bridgman's anvil leads to multiple cracking of the solid and its decomposition into individual particles. Intense compression and simultaneous deformation by shear forces are carried out in the temperature region of pre-melting of the crushed materials [10,11]. After HTSG, the output is a highly dispersed powder with a specific surface area of 0.1 to 10 m^2/g, depending on the type of polymer being ground. The considerable potential for the use of HTSG for processing and recycling of polymeric materials has been demonstrated by

* Corresponding authors.
E-mail addresses: sadush@icp.ac.ru (S.R. Allayarov), dadixon@ua.edu (D.A. Dixon).

https://doi.org/10.1016/j.polymdegradstab.2023.110631
Received 10 September 2023; Received in revised form 8 December 2023; Accepted 10 December 2023
Available online 14 December 2023

recent studies on the combined effect of γ-radiation and HTSG on the optical, surface-energy and thermophysical properties of γ-irradiated PE subjected to post-radiation grinding by the HTSG method [12,13]. However, there is no available information on the effect of radiation on the process of post-radiation HTSG of other polyolefins. This has prevented the determination of the extent to which this method of polymer reprocessing can be used. In the current work, we have investigated the HTSG of γ-irradiated industrial PP wastes for potential polymer recycling and to better understand the effects of high input radiation doses on the degree of functionalization of PP macromolecules.

Our approach to determining the effect of HTSG on γ-irradiated industrial PP wastes is to use infrared spectroscopy. There are significant differences between the characteristic IR spectra of isotactic and atactic PP IR absorption bands, such as the 1167, 997, and 841 cm^{-1} bands found in the spectrum of isotactic PP, which become very weak or disappear in the spectrum of atactic PP [14]. Thus, these bands are sensitive to the stereoisomerism of the PP chain [15–18] and changes in the intensities in the IR spectrum can be used to quantify the degree of PP micro-tacticity. Various methods for assessing the stereoisomeric composition of PP using IR spectroscopy are based on empirical relationships between the intensity of the above-mentioned individual bands and the degree of tacticity [7,8]. This is determined by the ratio of the number of isotactic triads to the total number of triads in the structure of PP macromolecules. In the current work, we use IR spectroscopy and computational chemistry to study the properties of products obtained by high-temperature shear grinding of initial and γ-irradiated samples of industrial PP.

2. Materials and methods

2.1. Materials

PP waste with mechanical damage due to manufacturing defects of the PPH007EX trademark produced by POLYOM LLC of the Omsk PP plant was used in the work. Most of the granules used in this study had a cylindrical shape with a diameter and height of 5 ± 1 and 2.5 ± 0.5 mm, respectively. They did not contain impurities.

2.2. γ-irradiation

Radiolysis by ^{60}Co γ-rays of PP samples was carried out in air using a UNU Gammatok-100 unit of the Federal Research Center for Problems of Chemical Chemistry and Medicinal Chemistry of the Russian Academy of Sciences at an input dose rate of 3 Gy/s. High input radiation doses were used to provide insights into how the polymer behaves under such dosing conditions as these are potentially relevant to polymer reprocessing as well as for polymer applications in high radiation fields.

2.3. High temperature shear grinding (HTSG)

Grinding of preliminarily γ-irradiated PP samples was carried out using special rotary dispersers at 200 ± 10 °C, the principle of operation of which in the mode of the so-called "continuous rheological explosion" is described in detail in [9–11,19]. During the experiment, the grinding temperature was set by heating the grinder housing with a ceramic annular clamp heater. Grinding of PP granules was carried out in a rotary disperser at a grinder screw speed of 0.6 s^{-1}. The diameter and length of the chopper screw are 32 and 350 mm, respectively. The length of the disperser rotor, where the melted polymer is crushed, is 110 mm. The resulting grinding product in the same rotor is subject to rapid water cooling at a rate of 90 °C/s. At the calculated speed of movement of granules along a helical line relative to the axis of the disperser cylinder of 60 mm/s, the time of passage of PP granules from the loading point to the disperser rotor was about 20 s. Before entering the rotor zone, the crushed PP granules were heated to 200 °C with an average heating rate ~9 °C/s while moving the loading zone up to the rotor. Thus, during the HTSG process, PP granules were heated from 27 °C to 200 °C in 20 s at a rate of about 9 °C/s.

2.4. IR spectral analysis

Spectroscopic analysis of PP samples in the mid-IR range (4000 cm^{-1} to 400 cm^{-1}) was carried out at room temperature on a Bruker ALPHA Fourier IR spectrometer equipped with an attenuated total internal reflection attachment with a single reflection diamond prism (ATR, FTIR-ATR). The spectral resolution was 4 cm^{-1} averaged over 25 scans per measurement. The degree of tacticity from the IR spectra of PP can be determined [8] by the intensity ratios of the following absorption bands: 974/1460 cm^{-1}, 974/1380 cm^{-1}, and 1380/1460 cm^{-1}. In samples of isotactic PP, the absorption bands at 973 and 997 cm^{-1} have the same intensity, whereas in the IR spectra of atactic PP, the band at 997 cm^{-1} is only a shoulder, and the intensity of the 973 cm^{-1} band remains the same [7]. As the 997 and 973 cm^{-1} bands are not directly correlated, they can be used for quantification of the isotactic ratio [20]. In the current work, the effect of the input dose of γ-irradiation on the stereoisomeric composition of industrial PP and the powder obtained by HTSG is determined by the ratio of the intensities of these two IR absorption bands (I_{997}/I_{973}) of the polymer.

2.5. Computational methods

We follow the approach we used to study the properties of polyethylene [12]. Molecular geometries of our model for the polymer were initially optimized at the density functional theory (DFT) level with the B3LYP functional [21,22] and DZVP2 basis set [23]. Frequencies were calculated to ensure that the geometry was an energetic minimum. The DFT optimized geometries were used as the starting geometries for calculations at the composite correlated G3(MP2)B3 molecular orbital theory level [24]. The G3(MP2)B3 composite correlated molecular orbital theory method [25] has been shown to provide reliable thermodynamic properties such as heats of formation and bond energies with errors on the order of 1 kcal/mol, at a reasonable computational expense for carbon-based systems. This is in contrast to most DFT functionals which exhibit larger errors [26]. All calculations were performed with Gaussian16 [27].

We benchmarked the G3(MP2)B3 method for a range of C—C, C—H, O—H, O—O, and C—O bond dissociation energies (BDEs) for compounds for which there are high quality experimental data from the Active Thermochemical Tables (ATcT) [28–31]. The Active Thermochemical Tables (ATcT) are based on a new paradigm of constructing, analyzing, and solving the underlying thermochemical network which defines the thermodynamic data incorporating the available experimental and computational data in a self-consistent manner with proper

Table 1
Bond dissociation enthalpies of model compounds at 0 K, ΔH(0 K), from G3(MP2)B3 and ATcT in kcal/mol.

Rxn	G3(MP2)B3	ATcT
$CH_4 \rightarrow {}^{\bullet}CH_3 + H^{\bullet}$	102.5	103.4 ± 0.0
$C_2H_6 \rightarrow CH_3^{\bullet}CH_2 + H^{\bullet}$	99.1	99.4 ± 0.1
$C_2H_6 \rightarrow 2\ {}^{\bullet}CH_3$	86.4	88.0 ± 0.1
$(CH_3)_3CH \rightarrow (CH_3)_2^{\bullet}CH + {}^{\bullet}CH_3$	85.7	86.4 ± 0.2
$(CH_3)_3CH \rightarrow (CH_3)_2CH^{\bullet}CH_2 + H^{\bullet}$	99.8	100.2 ± 0.3
$(CH_3)_3CH \rightarrow (CH_3)_3^{\bullet}C + H^{\bullet}$	95.2	94.9 ± 0.2
$HOO^{\bullet} \rightarrow H^{\bullet} + O_2$	48.1	48.0 ± 0.0
$HOOH \rightarrow H^{\bullet} + {}^{\bullet}OOH$	85.7	86.2 ± 0.1
$HOOH \rightarrow 2\ {}^{\bullet}OH$	46.3	48.8 ± 0.0
$CH_3OO^{\bullet} \rightarrow {}^{\bullet}CH_3 + O_2$	29.8	30.4 ± 0.1
$CH_3OOH \rightarrow CH_3OO^{\bullet} + {}^{\bullet}H$	84.3	84.5 ± 0.2
$CH_3OOH \rightarrow CH_3O^{\bullet} + {}^{\bullet}OH$	41.4	43.3 ± 0.2
$CH_3OOH \rightarrow {}^{\bullet}CH_3 + {}^{\bullet}OOH$	66.0	66.9 ± 0.2
$CH_3CH_2OOH \rightarrow CH_3^{\bullet}CH_2 + {}^{\bullet}OOH$	68.7	69.2 ± 0.4
$CH_3CH_2OOH \rightarrow CH_3CH_2O^{\bullet} + {}^{\bullet}OH$	41.2	43.4 ± 0.4

error propagation. The results show that the G3(MP2)B3 method provides excellent agreement with the best available data (Table 1).

3. Results and discussion

The degree of functionalization of a polymer after radiation can significantly affect the mechanism of HTSG as the surface energy, thermomechanical, and thermophysical properties of powders are changed [12,13]. To study the effect of the input dose of γ-irradiation on the degree of PP functionalization during radiation treatment and subsequent HTSG of the irradiated polymer, IR spectra of irradiated PP samples were obtained before and after HTSG.

3.1. PP granules γ-irradiated in air

The IR spectra of the original PP granules (a) and the granules (b, c, d) irradiated in air with different input doses are shown in Fig. 1; a shift along the ordinate axis is made for ease of comparison. In the IR spectrum of the unirradiated PP sample (a), four intense peaks are observed in the 3000–2800 cm^{-1} region and are assigned to the asymmetric (2950 cm^{-1}) and symmetric (2866 cm^{-1}) stretching vibrations of the C—H bonds in CH_3 groups and symmetric stretching (2838 cm^{-1}) and asymmetric (2917 cm^{-1}) vibrations of the C—H bonds in CH_2 groups. The spectrum also contains characteristic absorption bands assigned to the asymmetric (1454 cm^{-1}) and symmetric (1375 cm^{-1}) bending vibrations of the C—CH_3 group [32–34]. Fig. 2 shows the IR spectra of PP after grinding of granules exposed to various radiation input doses.

Radiolysis in air introduces significant changes in the IR spectrum of

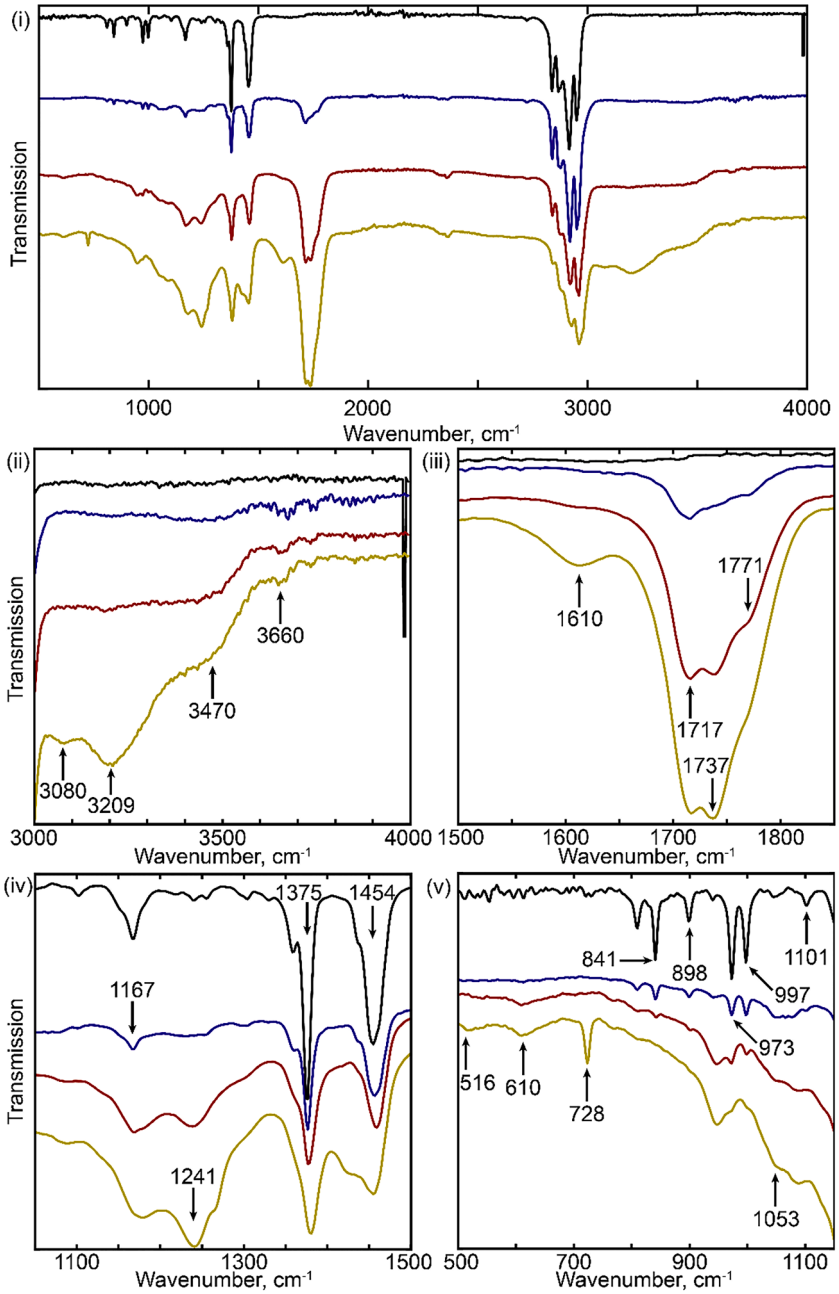

Fig. 1. IR spectra (i) and wavenumber of interest insets (ii-v) for non-irradiated (a, black) and γ-irradiated (in air) PP granules (b, blue = 1200 kGy, c, red = 8000 kGy, and d, yellow = 12,000 kGy).

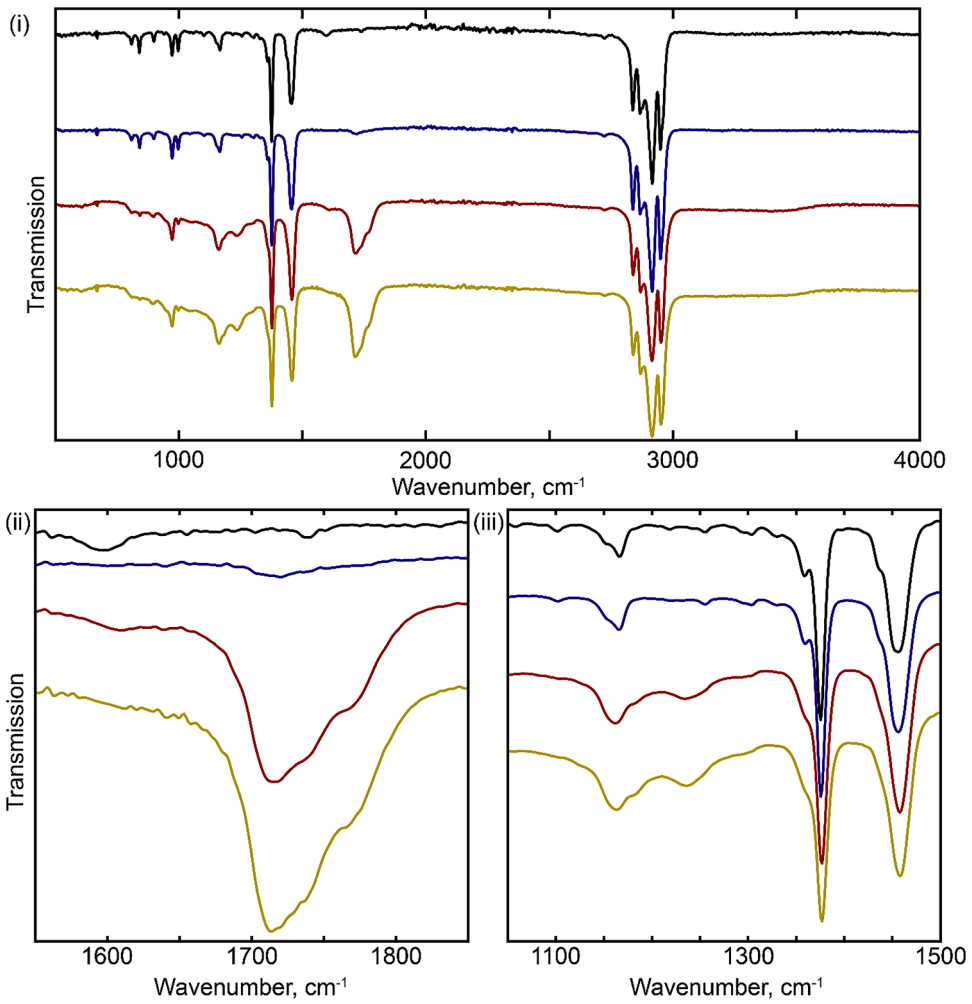

Fig. 2. IR spectra following HTSG (i) and wavenumber of interest insets (ii, iii) for non-irradiated (a, black) and γ-irradiated (in air) PP (b, blue = 1200 kGy, c, red = 8000 kGy, and d, yellow = 12,000 kGy).

the polymer. As a result of irradiation, the intensity and positions of individual absorption bands in the polymer change and new bands appear (Table 2). In the spectra of PP irradiated with different input doses (spectra b, c, d), an absorption band appears and grows in the region of 3690–3020 cm^{-1} with characteristic peaks at 3660, 3470, 3209, and 3080 cm^{-1} with increasing input dose of irradiation. The first three bands are assigned to stretching vibrations of OH groups, which are either free (3660 cm^{-1}) or involved in intermolecular and intramolecular hydrogen bonds (3470, 3209 cm^{-1}). The spectra also show a band in the region of 1820–1660 cm^{-1} formed by a group of three overlapping peaks (1771, 1737, 1717 cm^{-1}) corresponding to >C═O bond stretches, together with a peak at 1610 cm^{-1}, characteristic of C═C stretching vibrations of polyenes. Peaks at 1241, 1088, and 1053 cm^{-1} in the spectrum of irradiated granules confirm the presence of oxygen-containing groups. The peak at 1088 cm^{-1} is likely due to C—O absorption generated by reaction with oxygen or water and is likely a primary or secondary alcohol C—OH stretch but other C—O vibrations may provide a similarly broad peak at similar energy [35]. Peaks at 3080, 728, 610 and 515 cm^{-1} are characteristic of vinyl fragments –HC═CH_2 in the structure of irradiated PP.

As shown in Fig. 1 in the IR spectrum of the original sample of PP granules (a), the intensity of stretching vibrations of OH groups is ~0, and the intensity in this region is likely the result of atmospheric moisture. Analysis of the spectrum of irradiated PP, Fig. 1b–d, shows a small peak at 3660 cm^{-1} that assigned to a free OH group. Most of the hydroxyls resulting from irradiation are involved in intermolecular and intramolecular hydrogen bonds. The presence of hydrogen bonding leads to a decrease in the frequency of this vibration (bands at 3470 cm^{-1} and 3209 cm^{-1}). The OH stretches in gas and liquid H_2O are in the region of 3050–4000 cm^{-1} [36] with the gas phase bands at 3756 and 3657 cm^{-1} [37]. The bend of gas phase H_2O is at 1595 cm^{-1}, which is not observed in the IR spectra of γ-irradiated PP in Fig. 1.

The stretching vibration of the >C═O group in the frequency range 1745–1715 cm^{-1} tend to be narrow [33]. However, in the spectra of irradiated PP granules (Fig. 1b–d) this band is asymmetric and wide, since it consists of a superposition of at least three bands with maxima at 1717, 1737, and 1771 cm^{-1}. The intensity ratio of these three absorption bands changes with the radiation input dose. At radiation input doses up to 4000 kGy, the absorption band of carbonyl groups of aliphatic ketones (1717 cm^{-1}) has the highest intensity. As the input dose increases, the relative intensity of carbonyl absorption bands in the C(═O)O group of esters (1737 cm^{-1}) increases and there may be a small increase in the saturated γ-lactone band (1771 cm^{-1}) [38]. Thus, ketones are formed in PP granules irradiated with relatively low input doses. The amount of ketones formed as products of radiolysis decreases with irradiation input dose, and the formation of ester and acid groups increases. A similar superposition of the absorption bands of several oxygen-containing products was noted during the photooxidation of PP [39]. The reason for the appearance of hydroxyls, as well as fragments containing carbonyl groups in irradiated PP, is the radiation oxidation of PP by atmospheric oxygen and moisture.

The differences in the change of intensity of individual absorption

Table 2
IR absorption bands of PP before and after radiolysis by γ-rays of ^{60}Co and after high-temperature shear grinding (Powder).

Experimental IR transition, cm^{-1}					Lit. cm^{-1} [32–35]	Assignment[b]
Radiation input dose, kGy						
0 Pre-HTSG	4000	12,000	0 Post-HTSG	4000		
		3660			3670–3580	ν(O-H)
	3460	3470		3403m	3590–3400	ν(O-H)
	3204	3209		3200w	3200–2500	ν(O-H)
		3080			3150–3000	ν_{as}(-HC═CH_2)
		2980sh			3070–2930	ν_s(-HC═CH_2)
2961sh		2961 m	2961sh	2961sh	2975–2950	ν_{as} (–CH_3)
2950vs	2951 vs	2950sh	2950vs	2950vs	2975–2950	ν_{as} (–CH_3)
		2927 m			2940–2915	ν_{as} (–CH_2-)
2917vs	2920vs	2920sh	2917vs	2917vs	2940–2915	ν_{as} (–CH_2-)
2878sh	2878sh	2878m	2878sh	2878sh	2885–2865	ν_s (–CH_3)
2866s	2866sh		2866vs	2866 vs	2885–2865	ν_s (–CH_3)
2846sh		2846sh	2846sh	2846sh	2870 −2840	ν_s (–CH_2)
2838vs	2839s	2839	2838 vs	2838 vs	2870–2840	ν_s (–CH_2)
2724vw	2724vw	2724vw	2724vw	2724vw	2780–2680	ν(C—H)
		2365vw	2365vw	2365vw	2349.3	ν_{as}(O═C═O)
		2328vw			2325–2285	ν(C≡C)
	1761sh	1771 sh		1761sh		ν(C═O)
		1737vs	1737vw		1745–1715	ν(C═O)
	1717vs	1717vs		1717m	1745–1715	ν(C═O)
	1610sh	1610 m		1610vw	1625–1600	ν(>CH═CH-CH═CH<)
1460sh					1465–1440	δ_{as}(-CH_3)
1454s	1457s	1455s	1455s	1456s	1465–1440	δ_{as}(-CH_3)
	1436 sh	1436sh	1436sh	1436sh	1465–1440	δ_{as} (-CH_3)
		1380s			1390–1370	δ_s(-CH_3)
1375vs	1376vs	1380	1375vs	1375vs	1390–1370	δ_s(-CH_3)
1359sh	1359sh	1359sh	1359sh	1359sh	1365–1295	ω(CH_2)
1304vw	1304sh	1304sh	1304vw	1304vw	1305–1295	τ(CH_2) in -$(CH_2)_n$- (n>3)
1256vw		1256sh	1256vw	1256vw	1290–1200	τ(CH_2)
	1241 m	1241vs		1241vw	1265–1205	ν(C(O)—O)
1177sh	1177sh	1177s	1177sh		1195–1135	ρ(CH_3)
1167 m	1168 m	1168sh	1167m	1167 w	1160	ρ(CH_3)
1156sh	1156sh		1156sh			
1101vw	1101vw	1101sh	1101vw			
	1086m	1088m			1075–1000 /1150–1075 (1°/2°)	ν (C—OH) (1°/2°)
	1053vw	1053sh	1053vw		1055	ν_s(O-C═O)
1044vw		1044sh			1035–965	ρ(CH_3)
997 m	997vw	997vw	997m	997 w	1035–965	ρ(CH_3)
973 m	972vw	972vw	973m	973 w	970–910	ρ(CH_3)
940vw	948 m	948 m	940vw	940vw	970–910	ρ(CH_3)
898 w	898vw	898vw	898 w	898vw	1000–880	ρ(CH_3)
841 m	841vw	841vw	841m	841vw	841	ρ(CH_3)
809 w	809vw	809vw	809 w	809vw	809m	ρ(CH_3)
		728m		728vw	720–410	τ(CH_2) in CH═CH_2
	610vw	610m		610vw	720–410	τ(CH_2) in CH═CH_2
		515 w		515vw	600–250	

[a] Intensity of the absorption band: vs = very strong, *s* = strong, *m* = medium, *w* = weak, vw = very weak, sh = shoulder.
[b] ν = stretching, ν_s=symmetric stretching, ν_{as}=antisymmetric stretching, δ=bending, δ_s=symmetric bending, δ_{as}=antisymmetric bending, ρ=rocking, ω=wagging, τ=twisting.

bands depending on the irradiation input dose can be used to assess the effect of the input dose on the amount of the moieties responsible for these bands. Fig. 3 shows the dependence on the input dose of irradiation of the intensity of the absorption maxima of the C═O (curve a) and O—H (curve b) groups relative to the maximum of the absorption peak at 1375 cm^{-1}; the latter band is assigned to the C—CH_3 bond stretches (see Figs. 1 and 2). The band at 1375 cm^{-1} was chosen for normalization because its intensity remained nearly constant with respect to radiation input dose. An increase in the intensity of the peaks of oxygen-containing groups depending on the irradiation input dose is clearly apparent. These oxygen-containing peaks are due to radiolysis of the polymer in air. The intensity of the absorption peak of carbonyl groups linearly depends on the irradiation input dose up to 12,000 kGy. The absorption peak of hydroxyl fragments of irradiated granules also increases linearly with input dose but there is a discontinuity at ~5000 kGy. After an irradiation input dose of 12,000 kGy, the intensity of the absorption band of carbonyl groups at 1711 cm^{-1} in the IR spectrum of irradiated PP granules is six times higher than the intensity of the absorption band of hydroxyl fragments at 3470 cm^{-1}. The degree of change in the intensity of the peak characterizing the stretching vibrations of the hydrogen bonded OH group as a function of the irradiation input dose is lower than the change in the signal intensity of the C═O fragments. The main reason for this, most likely, is the structural feature of the monomer units of PP. Tertiary carbon atoms are present in the structure of each PP monomer unit, which contributes to easier radiation oxidation at this location, compared to polyolefins that do not have a tertiary carbon atom in the main chain. The relative intensity of the absorption band of carbonyl fragments of PP after irradiation is greater than the intensity of the bands after irradiation of polyethylene, which does not have a tertiary carbon atom in the main chain (Fig. 4, curves a, b). Fig. 4 (curve b) shows the dependence of the intensity of the C═O groups band (peak at 1705 cm^{-1}) on the input dose of irradiation of polyethylene granules [12]. The determination of the kinetics of the accumulation of ester fragments C(=O)O in PP with increasing

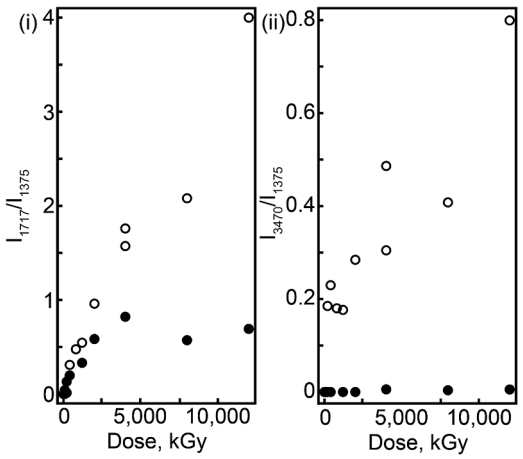

Fig. 3. Input dose dependence of PP irradiation of the relative intensity of the absorption bands (i) C═O (peak 1717 cm^{-1}) and (ii) OH (peak 3470 cm^{-1}) in samples of irradiated (in air) polymer granules (open circles) and in powder obtained after HTSG of irradiated (in air) granules (closed circles).

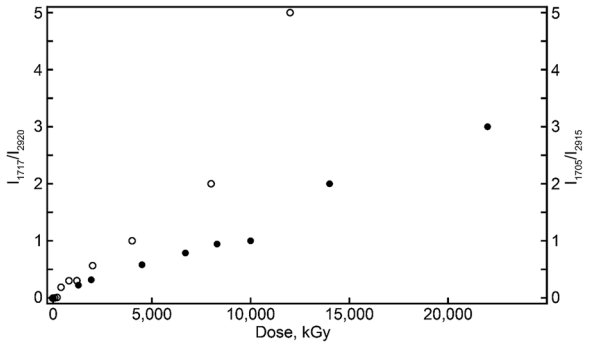

Fig. 4. Dependence of the intensity of the absorption band of >C═O groups on the input dose of irradiation (in air) of granules of PP (a, open circles, left y axis) and polyethylene (b, closed circles, right y axis) relative to the intensity of the absorption band of C—H bonds.

irradiation input dose from the IR spectra is complicated by the superposition of absorption bands in the region of 1241 cm^{-1}. Visual inspection of the spectra in Fig. 1 shows an increase in the intensity of the absorption band at 1241 cm^{-1} with an increase in the radiation input dose.

The gradient of changes in the low-intensity absorption peaks of various multiple bonds at 1610, 728, 610, and 515 cm^{-1} from the input dose of irradiation of PP granules is quite small, relative to changes in the IR signals of other chemical moieties created by radiation. The peaks assigned to these multiple π bonds are clearly observed only in the spectra of polymer granules irradiated with an input dose of 12,000 kGy. Thus, a comparison of the IR spectra of the granules of the original and γ-irradiated PP shows that during the radiolysis of PP in air, oxygen-containing groups and unsaturated bonds are formed and accumulated in the polymer macromolecules. Increasing the input dose leads to an increase in the content of radiation conversion products.

A characteristic feature of γ-irradiation of PP in air is the ease of oxidation of macromolecules of PP due to the presence of tertiary carbon atoms. By comparing the changes in the intensity of the absorption bands responsible for the CH, CH_2, and CH_3 fragments with the irradiation input dose, it is possible to estimate the degree of their participation in the radiative oxidation of PP macromolecules. However, the absorption frequencies of the C—H bond in the CH_2 fragment coincide with the absorption frequency of the same bond in the tertiary CH fragment. Therefore, using the intensity ratios I_{2920}/I_{2951} and assuming that the absorption cross-sections are the same, it was only possible to estimate the probability of breaking C—H bonds in CH_3 relative to breaking then in the $>CH_2$ and tertiary CH fragments taken together. The IR spectra of irradiated granules showed at irradiation input doses up to 8000 kGy that the value of I_{2920}/I_{2951} does not depend on the input dose and fluctuates with a value of 1.5 ± 0.1. This ratio is close to I_{2920}/I_{2951} = 1.5 in the IR spectrum of non-irradiated polymer granules. Consequently, upon γ-irradiation of PP in air, the probability of breaking C–H bonds in the side chain $–CH_3$ is comparable with the probability of C—H bond breaking in the $>CH_2$ and tertiary CH groups.

3.2. IR spectra of ground γ-irradiated PP

The granules retain their cylindrical appearance after irradiation at low input radiation doses. However, at higher input radiation doses, deformation of the surface of the granules (detected visually beginning at 4000 kGy) and a noticeable change in color (beginning at 2000 kGy) are observed. As radiation input dose increases, the initial white color of the polymer granules gradually changes to yellow then to light brown and dark brown as a result of the accumulation of various chromophores (C═O, C(═O)O, C═C) and auxochromic OH group in the granules (Table 2). The polymer granules gradually lose their initial hardness as irradiation input dose increases. At irradiation doses above 4500 kGy, the surface of the granules becomes sticky to the touch. This stickiness is not found following HTSG of the irradiated granules. This decrease in stickiness after HTSG may be due to the chemical moieties created by radiation and which are concentrated mainly on the surface of the granules, moving into the bulk of the powder or may accumulate inside the grinder. The result of this redistribution is a decrease in the concentration of chemical moieties created by radiation on the particle surface, leading to a significant reduction or loss of powder stickiness.

The powder particles obtained by HTSG of non-irradiated PP granules have an irregular shape in the form of fibers 1–2 mm long and 15–20 μm in diameter. γ-irradiation of polymer granules leads to a decrease in the particle size of the powder obtained by the grinding of the granules. Higher input doses of irradiation of the granules lead to smaller average particle sizes of the powders (Table 3). The powder obtained by grinding the non-irradiated granules has only 5 % of the powder particles with a size of less than 500 μm, whereas all particles of the powder obtained by HTSG of granules irradiated with an input dose of 850 kGy pass through a 500 μm sieve, and more than 90 % pass through a 200 μm sieve. Thus, increasing the input dose of preliminary γ-irradiation of the granules contributes to a marked reduction in the particle size of the powder obtained from HTSG.

Another feature of the irradiation of PP granules in air under our experimental conditions is that the depth of penetration of atmospheric oxygen into PP granules is extremely small. Consequently, the products obtained during the radiation oxidation of granules accumulate are not distributed homogeneously in the granules. For uniform oxidation of the entire polymer, the thickness of the sample must be less than the thickness of the oxidized layer (TOL). The TOLs of two polymers under the same radiation conditions are proportional to the square root of the permeabilities of the polymers [40]. We have previously shown that the

Table 3
Dependence on the irradiation input dose of the disperse composition of the powder obtained by grinding γ-irradiated PP granules.

Input dose, kGy	Sieve size, μm	Passed through sieve,%
0	500	5
	200	0
55	500	75
	200	40
450	500	90
	200	85
850	500	100
	200	90

TOL of polyvinylchloride (PVC) is ~ 11 μm for conditions typical to what is in use here [41]. Using the permeabilities for PVC and PP [42], we obtain an estimate for the TOL of ~ 40 μm for PP. If we account for the fact that the granules of the irradiated PP have a cylindrical shape with a diameter and height of 5 ± 1 and 2.5 ± 0.5 mm, then, during radiolysis in air, a small part of the volume, ~6 %, near the surface of the granules is irradiated in an oxidizing atmosphere. Therefore, during irradiation, especially at low input radiation doses, all products of radiation oxidation of PP granule macromolecules are concentrated in a narrow band near the surface. The interior of the granules are not oxidized.

The above features of the radiolysis of PP granules in air are manifested to varying degrees by changes in the absorption bands in the IR spectra of irradiated granules before and after grinding (Figs. 1 and 2). Most of the absorption bands in the spectra of irradiated granules (spectra b, c, d) are also in the spectra of the powder obtained after grinding (spectra f, g, h). In the spectrum of pre-irradiated PP followed by HTSG, there is a noticeable decrease in the intensity of the maxima of the peaks of oxygen-containing chemical moieties created by radiation at 1717 cm^{-1} (C═O band) and 1241 cm^{-1} (ν(C–O) in $CH_3C(=O)$–OR), as well as a decrease to almost zero in the intensity of the ν(O-H).band at 3470 cm^{-1}. The decrease in the intensity of these bands after grinding depends on the irradiation input dose. High irradiation input doses show stronger absorption peaks of oxygen containing chemical moieties created by radiation remain in the powders following HTSG. This trend is observed in the dependencies of the relative intensity of the maxima of the absorption peaks of C═O (Fig. 3(i)b) and OH fragments (Fig. 3(ii)b) in the spectra of powders on the irradiation input dose. The IR spectra of powders show that the proportions of these chemical moieties created by radiation sharply decrease relative to their proportion in the spectra of un-irradiated granules. After grinding the granules irradiated with an input dose of 12,000 kGy, the relative intensity of the C═O (1717 cm^{-1}), OH (3470 cm^{-1}) and C(=O)O (1241 cm^{-1}) bands decrease by factors of 6, 100, and 250, respectively.

There are two reasons for such changes in the IR spectra of the chemical moieties created by radiation. First, the IR spectra were taken in the ATR mode, which measures vibrations on the sample surface. As noted above, PP granules, exposed to irradiation, react with atmospheric oxygen and moisture only on the surface, because the diffusion of gases into the granules is limited [43,44]. Thus, the chemical bonds created during the radiation oxidation accumulate on the surface of the granules. The presence of oxygen in the reaction medium determines the course of radiation-chemical processes in the polymer. During HTSG, the irradiated granules are crushed, and the oxygen derived functional groups on the surface of the particles are distributed throughout the volume of the resulting powder leading to a nominally homogeneous mixture. Therefore, a decrease in the intensity of the maxima of the absorption bands of chemical moieties created by radiation accumulated on the surface of the granules may be a consequence of their redistribution over the entire volume of the resulting powder and will not be observed by a surface sensitive measurement. Secondly, HTSG involves heating the polymer to a melt temperature of 200 ± 10 °C, which can lead to thermal decomposition of chemical moieties created by radiation. To understand the processes occurring during such heating, experiments were carried out with gradual heating to 200 °C of PP samples irradiated in air to study the temperature dependence of the intensity of CSCR absorption peaks.

3.3. Temperature dependence of γ-radiation induced oxygenation of PP

IR spectra of irradiated granules heated to 45, 145 and 200 °C in the oven under air and then cooled to room temperature are shown in Fig. 5. The relative intensities of the signals of the skeletal groups of the polymer exhibit little dependence on the temperature within instrumental error. The intensities of stretching vibrations of the carbonyl, ester, and hydroxyl groups, Fig. 6 curves a-c respectively, decrease by a

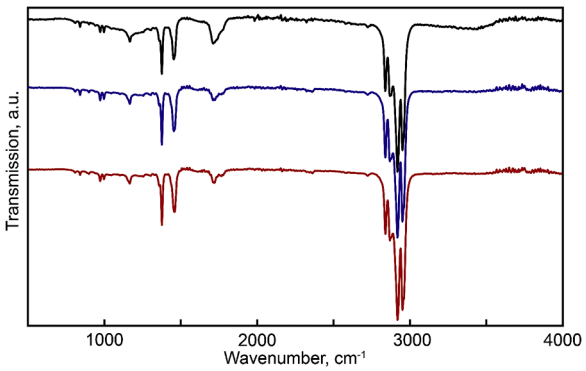

Fig. 5. IR Fourier spectra of PP granules irradiated with an input dose of 1000 kGy in air after heating to temperature (°C): 45 (a, black), 145 (b, blue), and 200 (c, red). Holding time at each temperature was 10 min.

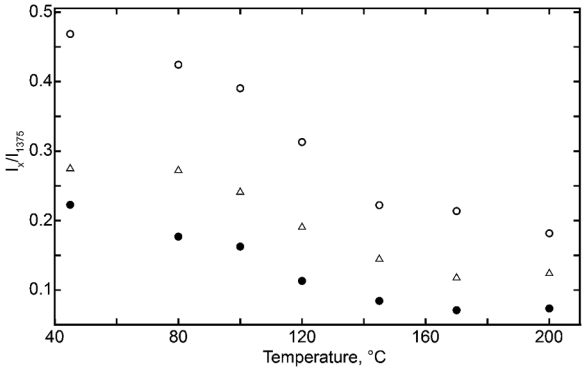

Fig. 6. Temperature dependence of the relative intensities of absorption bands in the IR spectrum in air-irradiated (1000 kGy) PP granules: ν(C=O) (a, 1737 cm^{-1}, open circles), ν(C–O) (b, 1241 cm^{-1}, open triangles), and ν(OH) (c, 3470 cm^{-1}, closed circles). Holding time at each temperature was 10 min.

factor of 2 to 3 with increasing temperatures up to 200 °C. This suggests the decomposition of these chemical moieties created by radiation upon heating irradiated polymer granules to 200 °C.

When describing the effect of heat on the polymer and CSCR during HTSG, the properties of the grinder must be accounted for. Before entering the rotor zone, the crushed PP granules are heated to 200 ± 10 °C at a heating rate of ~9 °C/s, for a total of ~20 s. Irradiated polymer granules heated in an oven demonstrated a noticeable decrease in the relative intensities of the absorption bands of oxygen-containing fragments at 80–100 °C; this decrease stops in the region of PP melting at temperatures near 160 °C (Fig. 6). Based upon these *ex situ* heating results, heating the polymer from 35 to 200 °C inside the disperser housing of the high-temperature shear grinder during grinding is accompanied by thermal decomposition of the chemical moieties created by radiation. As a result, the primary cause of the decreased absorption bands characteristic of chemical moieties created by radiation in powders obtained by grinding of irradiated granules is hypothesized to be thermal destruction of these moieties during grinding.

The influence of the heating duration on the relative intensity of the absorption bands of the studied chemical moieties created by radiation in the IR spectra of γ-irradiated granules was also studied. The results showed that lengthening of the heating time at 200 °C from 10 to 30 min does not affect the intensity of the absorption bands as shown in Fig. 7a–7c), i.e., the main processes leading to the attenuation of chemical moieties created by radiation signals during heating of irradiated granules occurs in the first 10 min of heating at 200 °C. It was also found that pressure treatment of 40 - 50 MPa does not lead to a change in the relative content of chemical moieties created by radiation in the

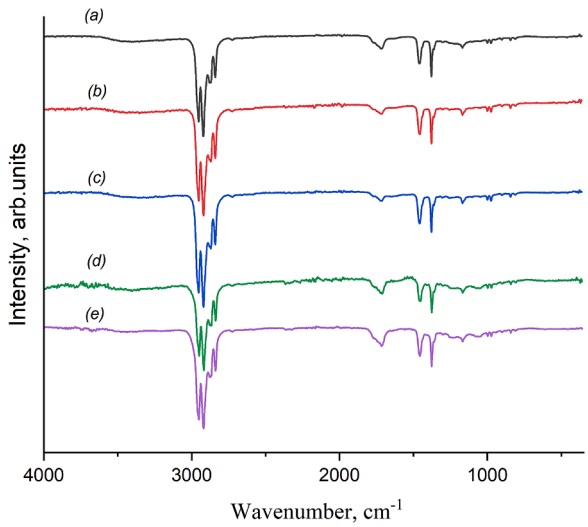

Fig. 7. IR spectra of PP granules irradiated in air with an input dose of 850 kGy before (a, black) and after exposure at 190 °C for 10 min (b, red) and 30 min (c, blue), as well as PP granules irradiated with an input dose of 1200 kGy before (d, green) and after pressing at room temperature under a pressure of 50 MPa (e, violet).

composition of the granules (Fig. 7d and e).

IR spectroscopy of the heated irradiated PP granules indicates a greater effect of temperature on the chemical moieties created by radiation composition during HTSG. Oxygenated fragments of PP macromolecules formed during radiolysis in air undergo thermal decomposition caused by heating to 200 ± 10 °C during HTSG. However, the heating time of the polymer sample in the HTSG process is not sufficient to thermally degrade the entire content of chemical moieties created by radiation in a single HTSG run. Therefore, in the IR spectra of powders obtained after one-time grinding of granules irradiated with large input doses, the IR signals for the remaining chemical moieties created by radiation are observed (Fig. 2c and 2d) and after grinding the granules irradiated with relatively low input doses that contain a smaller amount of these moietites, their absorption bands are absent in the spectra of the powders (Fig. 2b).

3.4. Ground PP γ-irradiated in vacuum

For practical applications, it is easier to carry out radiation treatments in air without the additional costs for vacuum or inert gases. Although irradiation in vacuum is less attractive from a practical point of view, it introduces less changes in the composition of the polyolefin than irradiation of the polymer in air as no oxygen or water is present. The effect of vacuum irradiation on their post-irradiation grinding was compared with the results for HTSG of granules irradiated in air. For vacuum irradiation, samples of PP granules were preliminarily pumped out in a vacuum degassing unit to a residual pressure of 0.13 Pa; the evacuated and sealed samples were then γ-irradiated.

Analysis of the IR spectra of unirradiated granules (Fig. 8a) and powder obtained by HTSG (Fig. 8b) shows that they are very similar with minor changes in relative intensities of some bands. Thus, under the conditions of HTSG, chemical processes do not occur and there is no significant change in the functional composition of the polymer. Slight changes are observed in the IR spectra of PP granules irradiated in vacuum pre- and post-grind, Fig. 8c and 8d respectively. As expected, irradiation of the polymer in vacuum, in contrast to irradiation in air, introduces only small changes in the IR spectrum.

Vacuum irradiation primarily forms fragments with terminal unsaturated bonds, a peak at 1656 cm^{-1}, and a broad band centered at 3340 cm^{-1} due to OH vibrations. The formation of hydroxyl substituents is likely due to small amounts of atmospheric water contamination adsorbed to the polymer during irradiation. Grinding of the irradiated granules leads to a decrease in the relative intensity of these two absorption bands. The band intensity of the chemical moieties created by radiation decreases as the polymer is ground multiple times as shown by comparing the spectra in Fig. 8d and 8e. After grinding five times, the bands for chemical moieties created by radiation nearly disappear in the spectrum, Fig. 7e. The decrease in the intensity of the 1656 cm^{-1} band due to HTSG is most likely due to the redistribution of chemical moieties created by radiation located on the surface of the irradiated granules throughout the entire volume of the powder as terminal unsaturation should be less susceptible to thermal degradation than the oxygen substituents. The hydroxyl groups likely decrease through a combination of both redistribution and thermal degradation.

3.5. γ-Irradiation induced stereoisomeric variation

The commercial PP granules used in this work were obtained using Ziegler–Natta catalysts, so the isotactic (methyl branches well-ordered on the same side of the polymer chain) polymer fraction dominates its composition. It has been demonstrated that high-energy radiation, which introduces defects into the polymer structure, can lead to a decrease in the degree of isotacticity of the polymer macromolecules. The ability for electron, ultraviolet, and γ-irradiation to partially racemize isotactic polymethyl methacrylate (PMMA) has been quantified [45,46]. To elucidate the effect of the γ-irradiation input dose on the stereoisomeric composition of PP granules and powders obtained during HTSG, changes in the intensities of IR absorption bands characteristic of the isotactic structure of PP were monitored. To assess the degree of

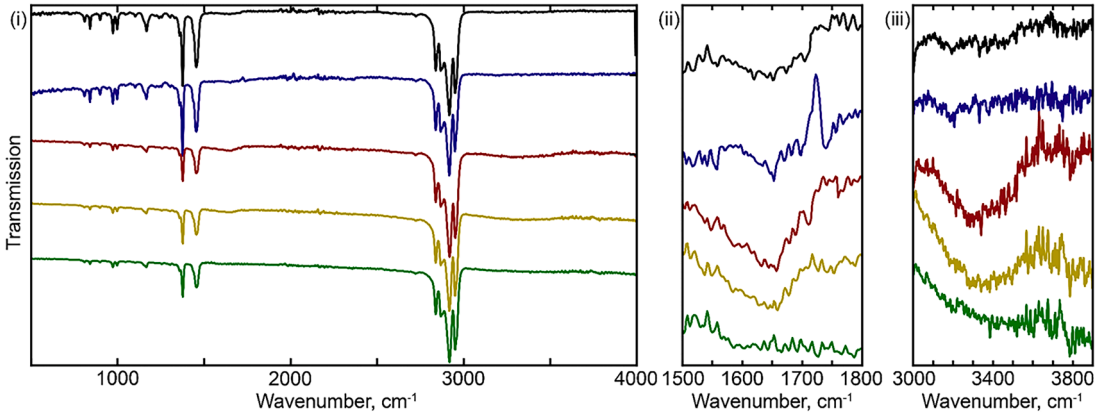

Fig. 8. IR spectra of unirradiated (a, black and b, blue) and irradiated in vacuum with an input dose of 850 kGy PP (c, red, d, yellow, and e, green) before (a, c) and after milling by the HTSG method by one-time (b, d) and five-fold milling (e).

isotacticity, we used the dependence of the relative intensity of the I_{997}/I_{975} absorption bands as representative of the content of the atactic fraction of the polymer given in [17]. The degree of tacticity of the initial PP granules is ~100 %, since $I_{997}/I_{975} = 0.97 \pm 0.07$, so the PP granules are mostly isotactic.

Fig. 9 shows the intensity ratio of the 973 and 997 cm^{-1} bands versus the irradiation input dose of PP granules for samples of irradiated granules before (curve a) and after (curve b) HTSG. Increasing the irradiation input dose decreases the relative intensity of the I_{977}/I_{973} ratio thereby decreasing the isotacticity of the PP. The I_{997}/I_{973} ratio for irradiated granules and the corresponding ground material are similar and both show a decrease with increasing input dose. This demonstrates that the primary reason for the loss of isotacticity of the polymer powders obtained by HTSG of irradiated granules is the preliminary γ-irradiation of the granules. This conclusion is consistent with the results of the analysis of the IR spectra of irradiated PP granules subjected to repeated HTSG. The ratio of the intensities of the 997/973 cm^{-1} bands of the spectra of PP granules irradiated with an input does of 850 kGy after a single (Fig. 8d) and after five-fold HTSG (Fig. 8e) do not change, so HTSG does not significantly impact the polymer isotacticity. The decrease in the isotacticity of the polymer sharply increases with a further increase in the irradiation dose of the granules. In the IR spectrum of granules irradiated with an input dose of 8000 kGy and the corresponding ground sample, the relative intensity of the peak at 997 cm^{-1} is nearly three times smaller than in the IR spectrum of non-irradiated granules and the corresponding powder. As a result, the degree of isotacticity of the latter with $I_{997}/I_{975} = 0.29 \pm 0.04$ can be calculated [17] to be ~13 %. The decrease in the degree of isotacticity upon irradiation leads to a decrease in the crystallinity of the recycled polymer. Such a decrease in the isotacticity of PP in powders obtained by HTSG of PP irradiated in air is mainly the result of the destruction of isotactic structures during γ-irradiation.

3.6. Mechanism of PP radiolysis

During γ-radiolysis of polyolefins, including PP, high energy photons impact the molecules leading to electronic excitations. Such electronic excitations have been studied extensively for alkanes in the ultraviolet (UV) and vacuum ultraviolet energy ranges [47–49]. As these are pure hydrocarbons with only single bonds, excitation is into antibonding C—C and C—H σ* orbitals which are dissociative in nature. Thus, the dominant photochemical processes will be bond breaking leading to the formation of radical species and in some cases ionization can occur. Recent work on UV absorption by isopentane supports the formation of neutral radicals via a uni-molecular photodissociation at 9.62 eV [49]. The ^{60}Co γ-radiation used in this work is much more energetic than UV light (1.17 and 1.33 MeV) [50] and can therefore photodissociate PP. The radicals that are formed can then undergo secondary reactions [51].

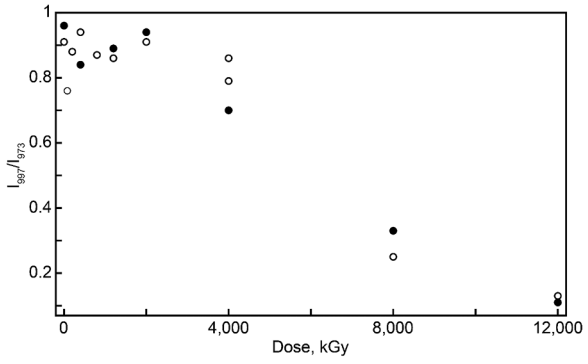

Fig. 9. Dependence of the intensity ratio of the absorption band at 997 cm^{-1} and 973 cm^{-1} on the input dose of irradiation in air of PP granules (a, open circles) and powder (b, closed circles) obtained by grinding irradiated granules.

Analysis of the products of radiolysis detected in the IR spectrum of irradiated PP indicates that the radiolysis of the polymer in air is a multipathway radical process with primary reactions being the formation of radicals or other active centers, which are subsequently oxidized by atmospheric oxygen.

The main processes that occur when polypropylene is exposed to γ-radiation under the conditions of our experiment are the following: 1) destruction of the main chain; 2) disproportionation; 3) formation of branches or cyclic structures due to reactions of inter- and intramolecular cross-linking; and 4) formation of oxygen-containing functional groups as a result of radiation-chemical oxidation of PP. In addition, post-irradiation in air HTSG has a significant effect on the chemical composition of the irradiated polymer products after grinding. Potential chemical processes leading to the formation of PP radiolysis products, determined from IR spectroscopy data, are presented below.

The breaking of C—C and C—H bonds with respective energies of ~90 and ~100 kcal/mol (Tables 1 and 4) is random when the polymer is irradiated with radiation from a ^{60}Co radioactive source with an energy of $1.2x10^6$ eV. However, when the polymer is irradiated, scattering and redistribution of the absorbed radiation energy along the long polymer chain can occur with a higher probability. As a result, bond breaking during radiolysis is more likely to occur at weak points near branches or structural irregularities. Some of the weakest bonds in PP are at tertiary carbons, where branching occurs, reactions (1) and (2). When the C—C bond of the PP main chain is broken (reaction (1)), two “terminal” alkyl radicals are formed, which may recombine due to the “cage effect”. The cage effect is recombination of radicals rather than bond dissociation due to mass transport limitations induced by both the solid phase and the long polymer chains associated with the radicals. The radicals can also disproportionate to form terminal unsaturated bonds (reactions (3) and (4)) which are highly exothermic or exit the cage, avoiding recombination. Although radical disproportionation, reactions (3) and (4), is thermodynamically similar to radical recombination, the negative of reaction (1), disproportionation has a hydrogen atom transfer energy barrier compared to the nominally barrierless radical recombination reaction which will slow disproportionation reaction kinetics compared to radical recombination. However, due to the relatively large size, separation of radicals formed by reactions (1) and (5) may not occur. Thus, the more probable reactions involve breaking of C–H bonds (reactions (5), (6), and (7)), or C–CH_3 scission (reaction (2)). The resulting low-molecular radical fragments can easily leave the polymer sites. Thus, in the matrix of this polymer during its low-temperature radiolysis, the so-called "middle" -$CH(CH_3)$-$C^{\bullet}H$-$CH(CH_3)$- and -CH_2-$C^{\bullet}(CH_3)$-CH_2-, as well as "side" macroradicals -CH_2-$CH(C^{\bullet}H_2)$-CH_2- can be formed [52]. As expected, formation of the radicals at the more substituted carbon, reaction (5), is more thermodynamically feasible than at the less substituted carbons, reactions (6) and (7) respectively. The resulting H atoms from radiolysis can abstract hydrogen atoms (reactions (8), (9), and (10)) to form H_2 or a methyl group to form methane (reaction (11)). The same radical formation trends that occur for hydrogen atom loss, reactions (5)-(7), persist for radical formation by hydrogen abstraction, reactions (8)-(10). Cleavage of a C—H bond and the formation of molecular hydrogen or other gaseous products are one of the main radiation-chemical processes of radiolysis of saturated alkanes [53] and their polymer analogs such as PP [43]. Disproportionation (reactions (3) and (4)) or other reactions leading to the release of radicals from the polymer are accompanied by degradation of the polymer chain. At the same time, the radicals that leave the polymer chain can carry away additional excitation energy, which can promote the decay of the resulting terminal radicals with the formation of low molecular weight alkenes (12) and (13).

It is also possible that the radicals can isomerize the radical center by H or CH_3 group transfers (reactions (14), (15), and (16)). The nature of the primary distribution of radicals in radiolyzed polyolefins can be masked by these isomerizations which can occur even at low temperatures as found for H transfers in PE [12]. In the same way,

Table 4
Polypropylene γ-radiation initiated degradation reaction thermodynamics at 298 K, in kcal/mol, calculated at the G3(MP2)B3 level.

Rxn #	Rxn	ΔH	ΔG
1		87.0	71.2
2	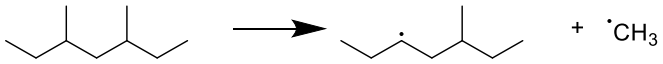	87.0	72.9
3	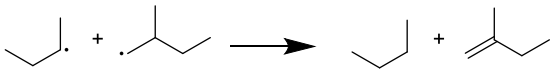	−68.6	−65.3
4	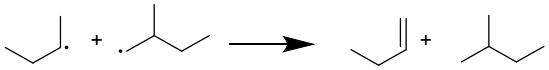	−66.6	−63.6
5		97.1	86.2
6	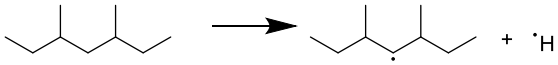	99.3	89.0
7	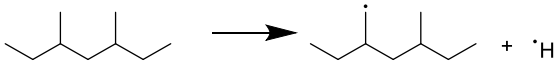	101.1	91.4
8	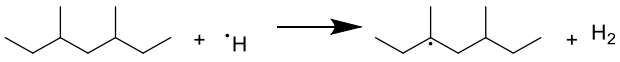	−8.2	−12.1
9	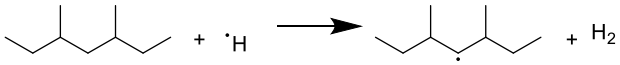	−6.0	−9.3
10	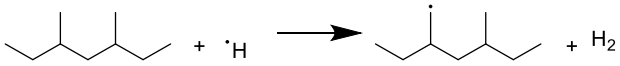	−4.2	−6.9
11	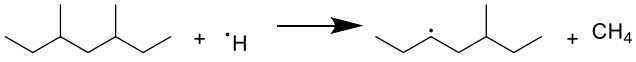	−17.1	−22.0
12	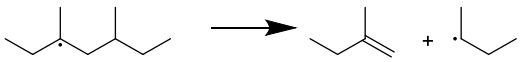	20.1	8.6
13	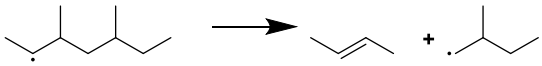	20.5	8.5
14	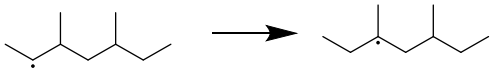	−1.8	−2.7
15	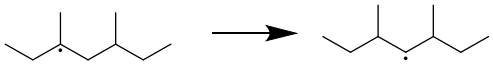	2.2	2.8
16	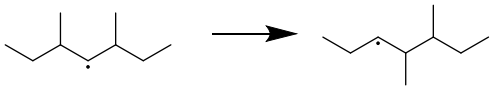	0.3	0.7
17	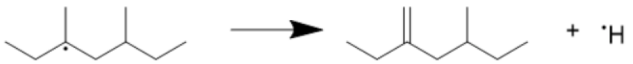	35.0	30.0

(*continued on next page*)

Table 4 (*continued*)

Rxn #	Rxn	ΔH	ΔG
18	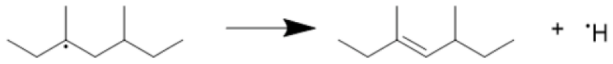	33.5	27.4
19	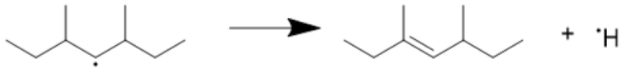	31.4	24.6
20		−70.3	−68.2
21	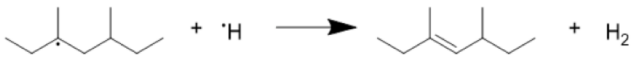	−71.7	−70.8
22	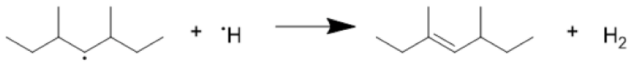	−73.9	−73.6
23	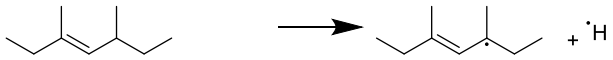	86.2	77.9
24	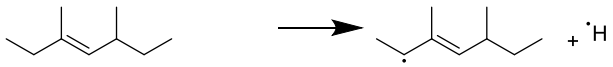	87.3	77.8

defect-stabilized radicals very easily transform into “middle” alkyl radicals [53]. Radical isomerization, radical disproportionation, and fragmentation of the chain into low-molecular-weight alkanes and polyolefins is most likely the reason why terminal radicals – C$^{\bullet}$H$_2$ have not been yet detected during solid-state radiolysis of polyolefins, even at −196 °C. Additional active sites involved in the radiation degradation of PP can be radicals conjugated with double bonds formed during the radiolysis of the polymer. Reactions leading to unsaturation caused by both bond dissociation (reactions (17)-(19)) and hydrogen abstraction (reactions (20)-(22)) were studied. As expected, formation of unsaturation along the PP backbone (reactions (18), (19), (21), and (22)) is thermodynamically preferred to unsaturation on the branching group (reactions (17) and (20)). Unsaturation starting with the radical β to the branching C is slightly lower energy than the reaction starting with the radical at the branching C. This is due to the lower BDE of the H at the branching carbon as stated prior. Following prior trends, hydrogen abstraction driven unsaturation (reactions (20)-(22)) is extremely exothermic and exergonic as two doublets are reacting to form two singlets. Once unsaturated C═C bonds form in PP, radiolysis can lead to loss of a hydrogen atom from the polymer molecule resulting in the formation of allylic radical centers (reactions (23) and (24)) and polyenyl radicals if conjugation is present. The differences in the C—H bond dissociations as represented by reactions (23) and (24) and those in reactions (5) to (7) of 10 to 15 kcal/mol are consistent with the allylic resonance energy of 12–13 ± 2 kcal/mol [54]. The allyl radicals formed by reactions (23) and (24) are characterized by different EPR spectra [44]. During heating of irradiated PP, the EPR spectra changes with the disappearance of nine lines from allyl radicals generated from reaction (23) to a spectrum with seven lines with a spacing of 1.5 mT from allyl radicals formed by reaction (24) [52]. This would suggest that the allyl radicals formed by reaction (24) are more thermally stable than the radicals formed by reaction (23) opposite to the predicted trend. This difference between computational thermodynamics and experimental values may be due to edge effects of the limited model molecule size.

The main products of PP radiation under oxidation conditions similar to the current experimental conditions are ketones, carboxylic acids, esters, tertiary hydroperoxide, dialkyl peroxide, tertiary alcohols, ketals, and hemiketals [55]. After the formation of various active centers during the radiolysis of PP, the next stage of radiation oxidation of the polymer is the reaction of radical centers with atmospheric oxygen. The resulting primary polymeric macroradicals (R) are rapidly oxidized with the formation of peroxide radicals with reactions (25) and (26) as examples.

$$CH_3 + O_2 \rightarrow CH_3OO \ (\Delta H(298\ K) = -31.4,\ \Delta G(298\ K) = -21.7\ kcal/mol) \quad (25)$$

$$C_2H_5 + O_2 \rightarrow C_2H_5O_2 \ (\Delta H(298\ K) = -34.2,\ \Delta G(298\ K) = -22.9\ kcal/mol) \quad (26)$$

The reactions of oxygen species are given in Table 5. The abstraction of an H atom from the polymer chain by $CH_3OO^{\bullet}$ is endothermic as shown by reactions (27) to (29). However, addition of O_2 to a macroradical to form a peroxy radical is exothermic as shown by reactions (30) and (31). Formation of a ketone by loss of $CH_3O^{\bullet}$ or $^{\bullet}OH$ as shown by reactions (32) and (33), respectively, is exothermic. Addition of O_2 β to the branch position is more exergonic than addition at the branch point, reactions (30) and (31) and subsequent loss of $^{\bullet}OH$ to form the ketone is more exothermic than the analogous loss of $^{\bullet}OCH_3$, reactions (32) and (33), indicating that formation of a ketone β to the branch location is the most favorable pathway. Reaction of the peroxy radicals to form peroxides is highly exothermic (reactions (34) and (35)), and if this reaction is coupled with the loss of $^{\bullet}OH$ (endothermic reactions (36) and (37)), the overall process to produce the oxy radical is still exothermic. The oxy radicals can cleave a C—C bond to produce a ketone or aldehyde, reactions (38) and (39). These have slightly positive enthalpies, but the free energies are negative due to the production of two product species. The reactions of the oxy radicals with an alkane to produce a hydroxy group (reactions (40) to (43)) are slightly exothermic. The ethane reactions, (42) and (43), are more favorable than the methane reactions, (40) and (41), due to the $CH_3C^{\bullet}H_2$ being more stable than the $^{\bullet}CH_3$ radical. Molecular oxygen O_2 can also insert into C—H bonds in alkenes in an exothermic process (reactions (44) to (46)). Insertion at the allylic position, reactions (44) and (45), is thermodynamically similar to addition to the unsaturation, reaction (46). The hydroperoxyl substituted alkenes can then disproportionate to form ketones or aldehydes and alcohols exothermically (reactions (47) to (49)). Molecular

Table 5
Oxygen reaction thermodynamics at 298 K in kcal/mol calculated at the G3(MP2)B3 level.

Rxn #	Rxn	ΔH	ΔG
27	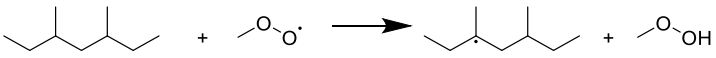	11.6	8.7
28	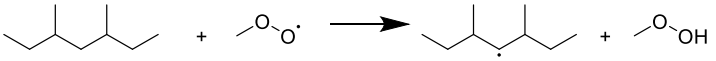	13.8	11.6
29	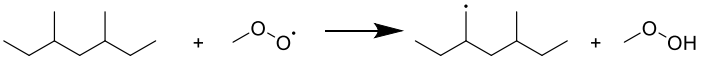	15.6	13.9
30	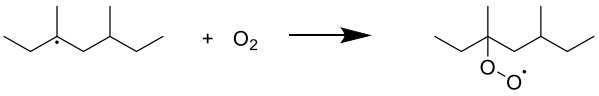	−36.3	−22.5
31	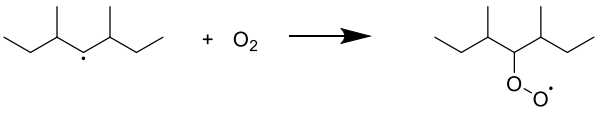	−36.5	−24.0
32	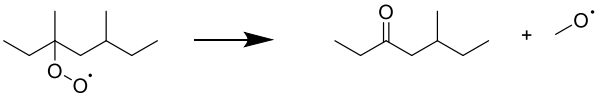	−26.2	−39.4
33	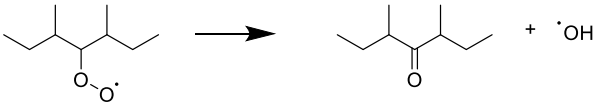	−29.3	−39.8
34	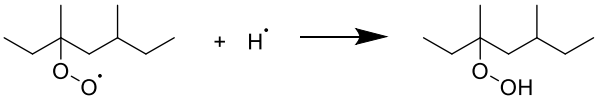	−87.4	−78.8
35	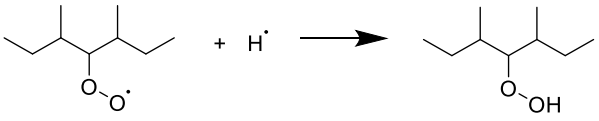	−83.3	−74.8
36	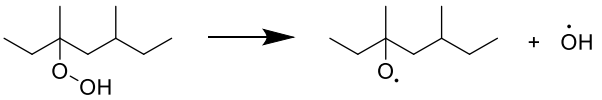	43.6	32.6
37	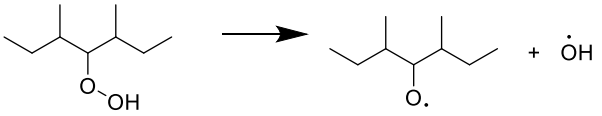	41.6	30.9
38	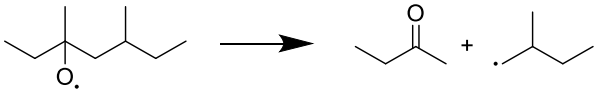	2.1	−12.8

(*continued on next page*)

Table 5 (*continued*)

Rxn #	Rxn	ΔH	ΔG
39	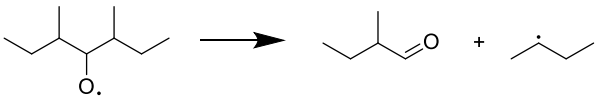	4.6	−9.9
40	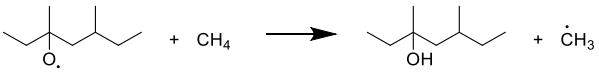	−0.4	−1.2
41	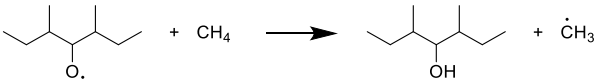	−1.0	−1.8
42		−3.7	−5.4
43	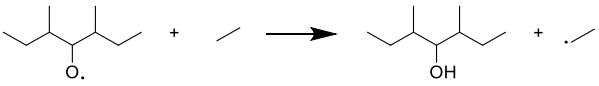	−4.2	−6.0
44	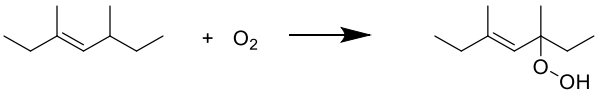	−20.4	−8.7
45	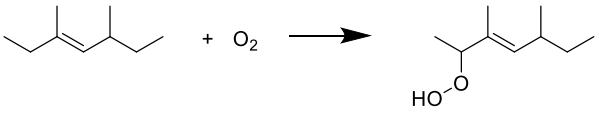	−21.4	−10.7
46	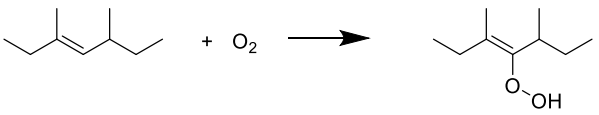	−21.4	−9.9
47	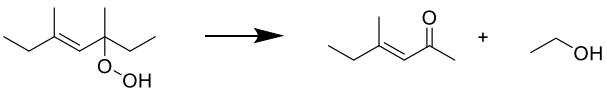	−52.5	−65.8
48	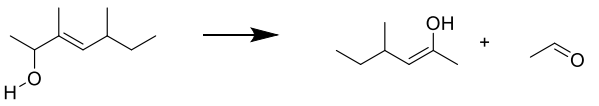	−50.1	−62.4
49	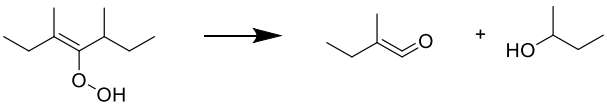	−45.2	−57.8
50	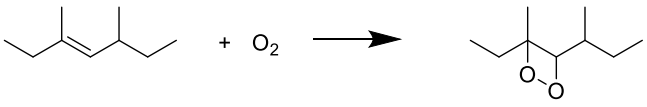	−18.9	−5.1
51	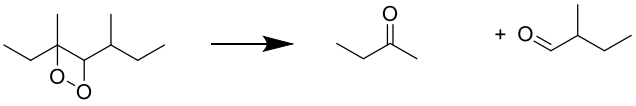	−63.8	−79.6

(*continued on next page*)

Table 5 (*continued*)

Rxn #	Rxn	ΔH	ΔG
52[a]	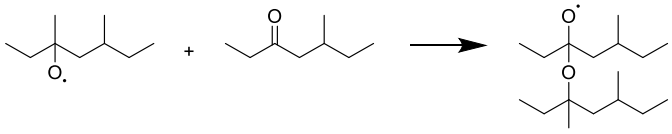	11.1	26.0
53[a]	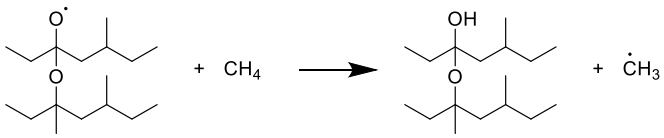	7.9	7.4
54[a]	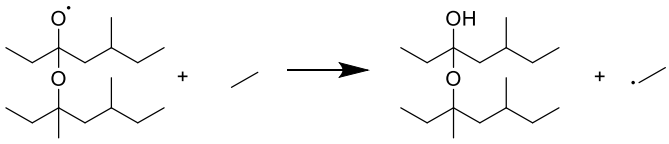	3.6	2.1

[a] Values calculated at B3LYP/DZVP2 level due to computational expense.

oxygen O_2 can also add across C═C double bonds in an exothermic process (reaction (50)) and then disproportionate (reaction (51)) to give an aldehyde and a ketone as well; both of these reactions are exothermic. Crosslinking of oxidized species and subsequent H abstraction is both endothermic and endergonic, reactions (52)-(54). Thus, as a result of radiation-chemical processes occurring during the oxidation of the primary radical products of PP radiolysis with atmospheric oxygen, various oxygen-containing derivatives of the polymer macromolecule and low molecular weight products are readily formed. Their appearance in the process of intramolecular transformations of irradiated PP is often accompanied by degradation of the polymer backbone. Consequently, radiolysis in air leads to the destruction of PP, despite the fact that this polymer can crosslink during radiolysis in vacuum [34].

4. Conclusions

Infrared spectroscopy and correlated molecular orbital theory computational chemistry were used to analyze polypropylene subjected to ^{60}Co γ-irradiation and post-radiation high-temperature shear grinding. The IR spectra of unirradiated PP granules and powder obtained by grinding granules shows that the species are the same, except for changes in the relative intensities of some absorption bands. Thus, the HTSG process does not introduce noticeable changes in the IR spectrum of the crushed polymer, i.e., there are no chemical processes occurring during grinding which lead to significant changes in the functional composition of the polymer. In the IR spectra of PP granules previously irradiated in vacuum, slight changes are observed related to the formation of fragments with terminal unsaturated bonds as well as hydroxyl fragments produced by contaminating water. Irradiation in vacuum allows for C═C unsaturation to form but does not allow for further reaction as nominally no O_2 or H_2O should be present. Grinding of the irradiated granules decreases the relative intensity of these bands, and after grinding five times, they decrease to negligible intensities.

Radiolysis in air introduces significant changes in the IR spectrum of the polymer granules with new oxygen-containing functional group and polyene vibrational bands appearing. As demonstrated in Table 5, polymer backbone reactions with either ambient O_2 or peroxy radicals formed *in situ* leads primarily to PP oxidation and chain destruction and is unlikely to lead to crosslinking. The intensity of the maximum absorption peak of carbonyl groups increases linearly with the input dose of irradiation up to 12,000 kGy of PP granules in air, and a similar increase in the intensity of the absorption peak of hydroxyl fragments is observed although there is a discontinuity at 5000 kGy. An asymmetric wide band for the carbonyl groups from 1715 to 1745 cm^{-1} consists of a superposition of at least three bands; the intensity ratios of these bands vary with radiation input dose. The variation in carbonyl vibrational frequency agrees well with the variety of carbonyl moieties found computationally, Table 5. At radiation input doses up to 2000 kGy, the absorption band of carbonyl groups of aliphatic ketones has the highest intensity. As the input dose increases, the relative intensity of carbonyl absorption bands of ester and lactone fragments increases. The intensity of the absorption peaks of unsaturated bonds is quite low, and they are clearly manifested only in the spectra of polymer granules irradiated with an input dose of 12,000 kGy. This lack of C═C bond formation at moderate irradiation input doses in air is well explained by the thermodynamic favorability of O_2 addition across unsaturation and subsequent spontaneous degradation of the resulting cyclic peroxide, Reactions (50) and (51) respectively.

The depth of penetration of oxygen into PP granules is small. During irradiation, especially at low input doses, all products of the radiation oxidation of macromolecules in granules are concentrated in a narrow surface region. During grinding, the irradiated granules are crushed leading to a nominally homogeneous mixture. This leads to a decrease in the intensity of the maxima of the absorption bands of some groups accumulated on the surface granules due to their redistribution over the entire volume of the ground powder. During the grinding by HTSG, the polymer granules are also heated to a melt temperature of 200 ± 10 °C, which can lead to thermal decomposition of chemical structures created by the radiation induced oxidation.

Most of the IR absorption bands of granules irradiated in air are also observed in the spectra of the powder obtained by grinding. In the spectrum of pre-irradiated and then ground PP, a noticeable decrease in the intensity of the absorption peak maxima of carbonyl containing fragments is observed, as well as almost a complete loss of hydroxyl vibration intensity. After grinding the granules irradiated with an input dose of 12,000 kGy, the relative intensities of the C═O, OH and C(=O)O absorption bands decrease by factors of ~ 6, 100 and 250 times, respectively. The analysis of the IR spectra of irradiated granules and their powder indicates a greater effect of heating on the composition of chemical structures created by radiation during grinding than simple spatial redistribution of bonds due to grinding.

The isotactic polymer fraction dominates in the current PP granules

and the fractions depend on the irradiation input dose. This fraction equally decreases as shown in the IR spectra of granules and powders obtained by grinding. The primary reason for the loss of isotacticity of polymer powders obtained from HTSG of irradiated granules is γ-irradiation of the granules as HTSG alone does not degrade the isotactic fraction. The loss of isotacticity is explained by production of methyl radicals by branching C—C bond cleavage and the nominally random orientation of methyl radical re-addition to PP backbone radicals.

With an increase in the input dose of radiation, the initial white color of the granules gradually changes to yellow, then to light brown and then dark brown due to the accumulation of various chromophore groups (C═O, C(═O)O, C═C) in the structure of the granules and the auxochromic group OH. PP granules gradually lose their primary hardness with increasing irradiation input doses. At input doses above 4000 kGy, the surface becomes very sticky to the touch. After grinding of the irradiated granules, there is a loss of stickiness in the powders. Even up to irradiation for more than 6.5 weeks at 3 Gy/s, the PP still retains many of its properties. It is only at this long irradiation time in air that formation of a large number of unsaturated bonds and oxygen-containing functionalized groups in a narrow surface region occurs. HTSG converts the irradiated PP into a material more like the parent as it mixes the degraded surface polymeric species with interior polymers with less radiation damage.

The powder particles produced after milling of non-irradiated granules are irregularly shaped in the form of fibers. Only 5 % of these particles are smaller than 500 μm. Preliminary γ-irradiation of polymer granules led to a decrease in the particle size of the powder. The higher irradiation input doses of the granules led to the formation the smaller average particle sizes of the powder. In the powder obtained after grinding of the granules irradiated with an input dose of 850 kGy, all particles pass not only through a 500 μm sieve, but more than 90 % of them pass through a 200 μm sieve. The decrease in final particle size and shape may be related to the stickiness of the irradiated material.

The combination of the experimental observations and the electronic structure calculations presented in this manuscript enabled an improved understanding of the mechanism of polymer degradation after γ-irradiation and high-temperature shear grinding. The possible application of γ-irradiation followed by HTSG to not only industrial waste PP but also to microplastic PP samples may provide a viable route forward for efficient microplastic recycling. High-temperature shear grinding of recycled polypropylene powder can lead to material with specified parameters and varying degrees of functionalization by varying the input dose and conditions of preliminary γ-irradiation prior to grinding. The recycling of PP using such an approach could enable saving primary raw materials and energy as the recycled PP may not be degraded that much in terms of its properties and quality, thus allowing the recycled PP to be used in a range of applications.

Supporting information

Total energies in a.u. and optimized Cartesian coordinates in Å.

CRediT authorship contribution statement

Sadulla R. Allayarov: Conceptualization, Data curation, Formal analysis, Funding acquisition, Investigation, Methodology, Writing – original draft, Writing – review & editing, Project administration. **Matthew P. Confer:** Data curation, Formal analysis, Investigation, Validation, Visualization, Writing – original draft, Writing – review & editing, Software. **Tatyana N. Rudneva:** Data curation, Formal analysis, Investigation, Validation, Visualization, Writing – original draft, Writing – review & editing, Methodology. **Sergei V. Demidov:** Data curation, Formal analysis, Investigation, Validation, Visualization, Writing – original draft, Writing – review & editing, Methodology. **Vadim G. Nikolskii:** Data curation, Formal analysis, Investigation, Validation, Visualization, Writing – original draft, Writing – review & editing, Methodology. **Svetlana D. Chekalina:** Data curation, Formal analysis, Investigation, Validation, Visualization, Writing – original draft, Writing – review & editing, Methodology. **David A. Dixon:** Conceptualization, Data curation, Formal analysis, Funding acquisition, Investigation, Methodology, Project administration, Resources, Supervision, Writing – original draft, Writing – review & editing, Software.

Declaration of Competing Interest

The authors declare no competing financial interest.

Data availability

The computational data is in the Supporting nformation. Experimental data will be made available on request.

Acknowledgments

This work was financially supported by the Russian state assignment AAAA-A19-119041090087-4 using the UNU "Gammatok-100″ of Federal Research Center of Problems of Chemical Physics and Medicinal Chemistry RAS. M. P. Confer acknowledges partial support from a National Science Foundation (NSF) Division of Ocean Sciences Postdoctoral Fellowship (2205819). D. A. Dixon thanks the Robert Ramsay Fund of The University of Alabama for partial support.

Supplementary materials

Supplementary material associated with this article can be found, in the online version, at doi:10.1016/j.polymdegradstab.2023.110631.

References

[1] E.P. Moore Jr., Polypropylene Handbook: Polymerization, Characterization, Properties, Processing, Applications, Hanser Publishers, Liberty Township, OH, USA, 1996, p. 419.
[2] D. Tripathi, Practical Guide to Polypropylene, iSmithers Rapra Publishin., Shawbury, UK, 2002, p. 104.
[3] J. Karger-Kocsis, T. Bárány, Polypropylene Handbook, Morphology, Blends and Composites, Springer, Cham, Switzerland, 2019, p. 641.
[4] R.R. Bora, R. Wang, F. You, Waste polypropylene plastic recycling toward climate change mitigation and circular economy: energy, environmental, and technoeconomic perspectives, ACS Sustain. Chem. Eng. 8 (2020) 16350–16363.
[5] R.E. Hester, R.M. Harrison, Marine Pollution and Human Health, Royal Society of Chemistry, Cambridge, UK, 2011, p. 184.
[6] M.A. Rakhimov, G.M. Rakhimova, E.M. Imanov, Problems of recycling polymer wastes, Fundam. Res. 8 (2014) 331–334.
[7] Federal classification catalog of waste electronic resource. (2023) https://rpn.gov.ru/fkko/?search=полипропилен (Accessed: 07/05/23) (in Russian).
[8] S. Antelava, S. Damilos, G. Hafeez, S.M. Manos, B.K. Al-Salem, K. Sharma, A. Kohli, Constantinou, plastic solid waste (PSW) in the context of life cycle assessment (LCA) and sustainable management, Environ. Manag. 64 (2019) 230–244.
[9] S.A. Wolfson, V.G. Nikolskii, Powder extrusion: fundamentals and different applications, Polym. Eng. Sci. 37 (1997) 1294–1300.
[10] S.A. Wolfson, V.G. Nikolskii, Solid-phase deformation fracture in the grinding of polymeric materials, Powder Technol. Vysokomol. Soedin. B 36 (1994) 1040–1041, in Russian.
[11] V.N. Balyberdin, V.G. Nikolsky, A.E. Arinstein, Dispergatory dlya tonkogo izmel'cheniya polimernykh materialov, kauchukov i kompozitov [Dispersants for fine grinding of polymeric materials, rubbers and composites], Tekhnol. Mashinostroyeniya 4 (1998) 94–101, in Russian.
[12] S.R. Allayarov, M.P. Confer, S.V. Demidov, G.V. Malkov, S.A. Bogdanova, I. F. Shaimukhametova, V.G. Nikolsky, Y.V. Perukhin, Y.V. Podvalnaya, I.V. Zyukin, D.A. Dixon, Joint influence of γ–irradiation and high temperature shear grinding on the IR spectra and surface–energy properties of polyethylene, Polymer 237 (2021), 124342.
[13] G.V. Malkov, S.V. Demidov, S.R. Allayarov, V.G. Nikol'skii, K.D. Semavin, A. T. Kapasharov, Y.V. Podvalnaya, Combined effect of high-temperature shear grinding and gamma-radiation on the thermal properties of polyethylene, High Energy Chem. 54 (2020) 130–135.
[14] A.G. Filimoshkin, N.I. Voronin, Khimicheskaya Modifikatsiya Polipropilena i Yego Proizvodnykh (Chemical Modification of Polypropylene and Its Derivatives), Tomskii Universitet, Tomsk, 1988, p. 180, in Russian.
[15] I. Ambrozh, L. Ambrozh, D. Belush, I. Dyachik, F. Janisch, Z. Manasik, A. Romanov, I. Rovner, D. Ryshchavy, K. Shishko, P. Shtirbany, F. Tomis, M. Fedelem,

Z. Forman, L. Freund, M. Jambrich, Polypropylen, Slovinské vydavateľstvo odbornej literatúry, 1964, pp. 208–215.
[16] Case Study FTIR For Identification Of Contamination. Report Template Jordi Inhouse J6264. (2014) https://jordilabs.com/wp-content/uploads/2014/09/Case_Study_FTIR_For_Identification_Of_Contamination.pdf (Accessed May 7, 2023).
[17] J.P. Luongo, Infrared study of polypropylene, J. Appl. Polym. Sci. 3 (1960) 302–309.
[18] Yu.V. Kissin, V.I. Tsvetkova, N.M. Chirkov, Opredeleniye stepeni izotaktichnosti polipropilena po yego infrakrasnym spektram [Determination of isotactic polypropylene at its infrared spectrum], Dokl. Akad. Nauk SSSR 152 (1963) 1162–1165, in Russian.
[19] V.G. Nikolskii, T.V. Dudareva, I.A. Krasotkina, U.G. Zvereva, V.G. Bekeshev, V. Ya. Rochev, A.M. Kaplan, N.I. Chekunaev, L.V. Vnukova, N.M. Styrikovich, I. V. Gordeeva, Development and properties of new nanomodifiers for road pavement, Russ. J. Phys. Chem. B 8 (2014) 577–583.
[20] T. Miyazawa, Y. Ideguchi, Molecular vibrations and structures of high polymers. V The infrared active normal vibrations of isotactic polypropylene, poly(propylene-2-d), poly(propylene-1,1-d2) and poly(propylene-3,3,3-d3) in the 1500~650 cm−1 Region, Bull. Chem. Soc. Jpn. 36 (1963) 1125–1141.
[21] A.D. Becke, Density-functional thermochemistry. III. The role of exact exchange, J. Chem. Phys. 98 (1993) 5648–5652.
[22] C.T. Lee, W.T. Yang, R.G. Parr, Development of the Colle-Salvetti correlation-energy formula into a functional of the electron density, Phys. Rev. B 37 (1988) 785–789.
[23] N. Godbout, D.R. Salahub, J. Andzelm, E. Wimmer, Optimization of Gaussian-type basis sets for local spin density functional calculations. Part I. Boron through neon, optimization technique and validation, Can. J. Chem. 70 (1992) 560–571.
[24] A.G. Baboul, L.A. Curtiss, P.C. Redfern, K. Raghavachari, Gaussian-3 theory using density functional geometries and zero-point energies, J. Chem. Phys. 110 (1999) 7650–7657.
[25] L.A. Curtiss, P.C. Redfern, K. Raghavachari, V. Rassolov, J.A. Pople, Gaussian-3 theory using reduced Mo/ller-Plesset order, J. Chem. Phys. 110 (1999) 4703–4709.
[26] P.C. Redfern, P. Zapol, L.A. Curtiss, K. Raghavachari, Assessment of Gaussian-3 and density functional theories for enthalpies of formation of C_1−C_{16} alkanes, J. Phys. Chem. A 104 (2000) 5850–5854.
[27] M.J. Frisch, G.W. Trucks, H.B. Schlegel, et al., Gaussian 16, Revision A.03, Gaussian, Inc., Wallingford CT, 2016, Gaussian, Inc., Wallingford CT, 2016.
[28] B. Ruscic, D.H. Bross, Active thermochemical tables (ATcT) values based on ver. 1.124 of the thermochemical network (2023); available at https://atct.anl.gov/Thermochemical%20Data/version%201.124/index.php. (Accessed July 5, 2023).
[29] B. Ruscic, R.E. Pinzon, M.L. Morton, G. von Laszewski, S.J. Bittner, S.G. Nijsure, K. A. Amin, M. Minkoff, A.F. Wagner, Introduction to active thermochemical tables: several "key" enthalpies of formation revisited, J. Phys. Chem. A 108 (2004) 9979–9997.
[30] P.B. Changala, T.L. Nguyen, J.H. Baraban, G.B. Ellison, J.F. Stanton, D.H. Bross, B. Ruscic, Active thermochemical tables: the adiabatic ionization energy of hydrogen peroxide, J. Phys. Chem. A 121 (2017) 8799–8806.
[31] D.H. Bross, B. Ruscic, Chapter 1 – Thermochemistry, in: Computer Aided Chemical Engineering, 45, Elsevier, 2019, pp. 3–114.
[32] K. Abe, K. Yanagisawa, Spectra of melted polypropylene film, J. Polym. Sci. 36 (1959) 536–539.
[33] G. Socrates, Infrared and Raman Characteristic Group Frequencies Tables and Charts, 3rd ed., John Wiley & Sons, Inc., New York, 2004, p. 368.
[34] C.Y. Liang, F.G. Pearson, Infrared spectra of crystalline and stereoregular polymers: part I. Polypropylene, J. Mol. Spectrosc. 5 (1961) 290–306.
[35] D. Lin-Vien, N.B. Colthup, W.G. Fateley, J.G. Grasselli, The Handbook of Infrared and Raman Characteristic Frequencies of Organic Molecules, Elsevier, 1991, p. 46.
[36] NIST Chemistry WebBook (2023) (https://webbook.nist.gov/chemistry) (Accessed May 7, 2023).
[37] T. Shimanouchi. Tables of Molecular Vibrational Frequencies, Consolidated Volume 1. NSRDS-NBS 39, U.S. Government, Washington DC, 1972 160 pp.
[38] R.N. Jones, B.S. Gallagher, The infrared spectra of steroid lactones, J. Am. Chem. Soc. 81 (1959) 5242–5251.
[39] Y. Zhou, B. Li, P. Zhang, Fourier transform infrared (FT-IR) imaging coupled with principal component analysis (PCA) for the study of photooxidation of polypropylene, Appl. Spectrosc. 66 (2012) 566–573.
[40] D.W. Clegg, A.A. Collyer, Irradiation Effects on Polymers, 1st ed., Springer, 1991, pp. 157–223. Elsevier Applied Science.
[41] S.R. Allayarov, M.P. Confer, S.A. Bogdanova, T.N. Rudneva, U.Yu. Allayarova, I. F. Shaimukhametova, S.V. Demidov, D.V. Mishchenko, E.N. Klimanova, T. E. Sashenkova, S.D. Chekalina, S.M. Aldoshin, D.A. Dixon, Characteristics and radiolysis behavior of polyvinylchloride under accelerated proton and γ-irradiation, Radiat. Phys. Chem. (2022), 110436.
[42] L. Bastarrachea, S. Dhawan, S.S. Sablani, Engineering properties of polymeric-based antimicrobial films for food packaging, Food Eng. Rev. 3 (2011) 79–93.
[43] J.E. Wilson, Radiation Chemistry of Monomers, Polymers and Plastics, Marcel Dekker Inc., 1974.
[44] F.W. Shen, H. McKellop, Interaction of oxidation and crosslinking in gamma irradiated ultra-high molecular weight polyethylene, J. Biomed. Mater. Res. 61 (2002) 430–439.
[45] E.V. Thompson, Electron irradiation and racemization of isotactic poly(methyl methacrylate), Polym. Lett. 3 (1965) 675–678.
[46] C. David, A. Verhasselt, G. Geuskens, Racemization of isotactic polymethylmethacrylate by ultra-violet and gamma irradiations, Polymer 9 (1968) 287–288.
[47] J.W. Raymonda, W.T. Simpson, Experimental and theoretical study of sigma-bond electronic transitions in alkanes, J. Chem. Phys. 47 (1967) 430–448.
[48] J.W. Au, G. Cooper, G.R. Burton, T.N. Olney, C.E. Brion, The valence shell photoabsorption of the linear alkanes, C_nH_{2n+2} (n=1-8): absolute oscillator strengths (7-220 eV), Chem. Phys. 173 (1993) 209–239.
[49] A.K. Das, K. Sunanda, B.N. Rajaskehar, Spectroscopy of structural isomers of pentances: an experimental and theoretical study, J. Mol. Struct. 1245 (2021), 131126.
[50] G. Lindström, A. Hedgran, D.E. Alburger, Precision measurement of Co^{60} gamma-radiation, Phys. Rev. 89 (1953) 1303–1304.
[51] M. Dole, The Radiation Chemistry of Macromolecules, Academic Press, 1972.
[52] S.Ya. Pshczhctskii, A.G. Kotov, V.K. Milinchuk, V.A. Roginskii, V.I. Tupikov, EPR of Free Radicals in Radiation Chemistry, John Wiley & Sons, New York, 1974, p. 446.
[53] V.V. Saraeva, Radiolysis of Hydrocarbons in the Liquid Phase, Publishing House of Moscow State University, Moscow, 1986 in Russian.
[54] W.E. von Doering, G.H. Beasley, Delocalization Resonance energy of the allylic radical from the geometrical isomerization of hexa-1,3,5-trienes, Tetrahedron 29 (1973) 2231–2243.
[55] R. Bernstein, S.M. Thornberg, R.A. Assink, D.M. Mowery, M.K. Alam, A.N. Irwin, J. M. Hochrein, D.K. Derzon, S.B. Klamo, R.L. Clough, Insights into oxidation mechanisms in gamma-irradiated polypropylene, utilizing selective isotopic labeling with analysis by GC/MS, NMR and FTIR, Nucl. Instrum. Methods Phys. Res. Sect. B 265 (2007) 8–17.